Nonvalence Correlation−Bound Anion States of Spherical Fullerenes

ARTICLE *in* NANO LETTERS · JUNE 2014

Impact Factor: 13.59 · DOI: 10.1021/nl5016574 · Source: PubMed

2 AUTHORS:

Vamsee Voora
University of Pittsburgh
11 PUBLICATIONS **149** CITATIONS
SEE PROFILE

Kenneth D Jordan
University of Pittsburgh
372 PUBLICATIONS **13,939** CITATIONS
SEE PROFILE

NANO LETTERS

Letter

pubs.acs.org/NanoLett

Nonvalence Correlation-Bound Anion States of Spherical Fullerenes

Vamsee K. Voora and Kenneth D. Jordan*

Department of Chemistry and Center for Molecular and Materials Simulations, University of Pittsburgh, Pittsburgh Pennsylvania 15260, United States

Supporting Information

ABSTRACT: We present a one-electron model Hamiltonian for characterizing nonvalence correlation-bound anion states of fullerene molecules. These states are the finite system analogs of image potential states of metallic surfaces. The model potential accounts for both atomic and charge-flow polarization and is used to characterize the nonvalence correlation-bound anion states of the C_{60}, $(C_{60})_2$, C_{240}, and $C_{60}@C_{240}$ fullerene systems. Although C_{60} is found to have a single (s-type) nonvalence correlation-bound anion state, the larger fullerenes are demonstrated to have multiple nonvalence correlation-bound anion states.

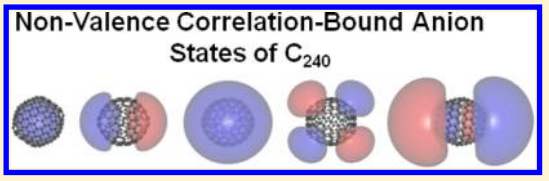

KEYWORDS: *Nonvalence correlation-bound anions, equation-of-motion coupled-cluster theory, electron binding, image potential states, charge-flow polarizability, fullerenes*

Bound anion states of molecules and clusters can be classified as valence-bound, electrostatically-bound, or nonvalence correlation-bound depending on the nature of interaction between the excess electron and the molecule. In valence-bound anion states, the excess electron is bound by short-range interactions, while in electrostatically bound anion states, it is bound primarily through interactions with the permanent multipole moments of the molecule(s). In nonvalence correlation-bound anion states, which are the topic of this paper, long-range dispersion-type correlation interactions are essential for the binding of the excess electron.[1−3] By definition, correlation-bound anions states are not bound at Hartree−Fock (HF) level of theory and thus require the use of theoretical methods that do not depend on the HF method providing a suitable starting wave function. The existence of such anion states has been established for sufficiently large $(Xe)_n$ clusters,[2] certain $(H_2O)_n$ clusters,[4] and, more recently, for C_6F_6[5] and the C_{60} fullerene.[3] Scanning tunneling microscopy (STM) and two-photon photoemission studies of C_{60} and C_6F_6 on the Cu(111) surface provide evidence for very diffuse anionic states of the absorbed molecules[6−9] that we have attributed to nonvalence correlation-bound anion states.[3,5] The orbitals involved in electron capture to give such anions are sometimes referred to as "superatom molecular orbitals".[7,8,10] In our work on the nonvalence correlation-bound anion states of C_6F_6 and C_{60}, the main theoretical approach was the ab initio electron attachment equation-of-motion coupled-cluster singles-doubles (EA-EOM-CCSD) method,[11] which due to computational demands cannot be used for fullerenes much larger than C_{60}. A common characteristic of nonvalence correlation-bound anion states is that the orbital occupied by the excess electron is very extended, which suggests the possibility of accurately chracterizing these species by use of a model Hamiltonian approach with the excess electron being treated quantum mechanically and the electrons of the neutral molecule being described by means of an effective potential. Such an approach is similar in spirit to that used by Warshel and Karplus for treating conjugated π-electron molecules. In their approach, the π-electrons are treated explicitly, while the effect of the σ electrons is accounted by means of an empirical potential.[12]

In this work, we present a one-electron model Hamiltonian for characterizing nonvalence correlation-bound anion states of fullerenes. This is an extension of a model Hamiltonian approach that we recently introduced to characterize excess electrons interacting with water clusters.[13] The model employs a polarization potential within the context of the adiabatic approximation to account for the long-range dispersion interactions between the excess electron and the molecules.[14] Fullerenes have much smaller one-particle band gaps than water, imparting them with partial metallic character. As a result, their nonvalence correlation-bound anion states can be thought of as counterparts to image-potential states of metallic surfaces,[15−18] making it important to include charge-flow polarizability in addition to atom centered point-inducible dipoles.[19−24] The charge-flow polarization allows for the readjustment of the atomic charges due to the electric field of the point electron. Although model potentials have been used in the past to search for nonvalence anion states of C_{60},[25−28] these earlier studies used simpler models of the electrostatics, polarization, and short-range repulsive interactions than employed in the present study. We apply the resulting model Hamiltonian to characterize the nonvalence correlation-bound anion states of the C_{60}, $(C_{60})_2$, C_{240}, and $C_{60}@C_{240}$ fullerene systems. The C_{60} and C_{240} fullerenes have a hexicosahedral

Received: May 3, 2014
Revised: June 21, 2014
Published: June 30, 2014

   dx.doi.org/10.1021/nl5016574 | *Nano Lett.* 2014, 14, 4602−4606

symmetry, while $C_{60}@C_{240}$ is comprised of a C_{60} fullerene encapsulated inside the C_{240} fullerene.

The Hamiltonian describing the interaction of the excess electron with the fullerene is

$$\hat{H}^{\mathrm{el}}(\mathbf{r}) = \hat{T}^{\mathrm{el}}(\mathbf{r}) + \hat{V}^{\mathrm{el-fullerene}}(\mathbf{r}) \tag{1}$$

where $\mathbf{r}$ is the vector denoting the position of the electron, $\hat{T}^{\mathrm{el}}$ is the kinetic energy operator and $\hat{V}^{\mathrm{el-fullerene}}$ is the potential energy operator which consists of electrostatic, repulsion, and polarization terms

$$\hat{V}^{\mathrm{el-fullerene}}(\mathbf{r}) = V_{\mathrm{es}}(\mathbf{r}) + V_{\mathrm{rep}}(\mathbf{r}) + V_{\mathrm{pol}}(\mathbf{r}) \tag{2}$$

The electrostatic potential, V_{es}, is modeled by atom-centered point dipoles

$$V_{\mathrm{es}}(\mathbf{r}) = -\sum_{i}^{N} \frac{\mu_i \cdot \mathbf{R}_{ie}}{R_{ie}^{3}} \tag{3}$$

where μ_i is the atomic dipole moment at the ith site, $\mathbf{R}_{ie}$ is the vector between the ith site located at $\mathbf{R}_i$ and the electron at $\mathbf{r}$, $R_{ie} = |\mathbf{R}_{ie}|$ and N is the number of atoms. For a graphene sheet, the leading atomic multipole moment is the quadrupole. However, for curved fullerene surfaces a distributed multipole analysis[29] of the charge-distribution gives finite atomic dipoles perpendicular to the surface. Although quadrupole and higher atomic multipole moments are non-negligible, we retain in the model only the atomic dipoles, fitting them to best represent the ab initio electrostatic potential at the center of the fullerene of interest. The resulting atomic dipoles are 0.0597 and 0.0245 D for C_{60} and C_{240}, respectively.

The repulsive potential accounts in an effective manner for exchange interactions between the excess electron and the electrons of the carbon atoms as well as for orthogonalization and charge-penetration[30] effects. We express the repulsive potential in terms of an s-type Gaussian function on each carbon atom

$$V_{\mathrm{rep}}(\mathbf{r}) = \sum_{i}^{N} a \exp(-bR_{ie}^{2}) \tag{4}$$

where the summation is over the C atoms.

The final term in eq 2 is the polarization potential which incorporates the interaction of the excess electron with the induced moments resulting from the field from the electron on the fullerenes as well as from the interactions between fullerene molecules

$$\begin{aligned} V_{\mathrm{pol}}(\mathbf{r}) &= -(\mathbf{F}^{\mathrm{e}}(\mathbf{r}))^{\mathrm{T}} \cdot \alpha^{\mathrm{fullerene}} \cdot \left(\frac{1}{2}\mathbf{F}^{\mathrm{e}}(\mathbf{r}) + \mathbf{F}^{\mathrm{fullerene}}\right) \\ &= -(\mathbf{F}^{\mathrm{e}}(\mathbf{r}))^{\mathrm{T}} \cdot \mathbf{M}^{\mathrm{ind}} \end{aligned} \tag{5}$$

where $\mathbf{F}^{\mathrm{e}}$ is a supervector consisting of potentials, $\mathbf{V}^{\mathrm{e}}$, and electric fields, $\mathbf{E}^{\mathrm{e}}$, on the atoms of the fullerenes due to the electron, and $\mathbf{F}^{\mathrm{fullerene}}$ is a supervector that accounts for the potentials and fields between the fullerenes. $\alpha^{\mathrm{fullerene}}$ is the polarizability matrix of the fullerene(s) and accounts for both charge-flow and atom-centered point inducible dipoles. $\mathbf{M}^{\mathrm{ind}}$ is a supervector consisting of the induced charges, $\mathbf{q}$ (due to charge-flow) and the induced dipoles, μ, on the atomic sites. (See Supporting Information for details on $\alpha^{\mathrm{fullerene}}$ and $\mathbf{M}^{\mathrm{ind}}$.) The one-electron Schrödinger equation is solved using a discrete variable representation (DVR) grid-type basis set[31] as implemented in the PISCES code[32] developed in our group for describing nonvalence excess electron systems.

The model potential described above was used to characterize the nonvalence correlation-bound anionic states of C_{60}, C_{240}, $(C_{60})_2$, and $C_{60}@C_{240}$. For C_{60}, the model Hamiltonian gives a single s-type nonvalence correlation-bound anion state with an electron binding energy (EBE) of 0.13 eV, which, because of the use of this species in determining the parameter in the damping function for the polarization potential, is essentially identical to the EOM-CCSD result (we are using the sign convention that a positive EBE corresponds to a bound anion. In addition, with the geometries used +EBE corresponds to a vertical electron affinity). The orbital occupied by the excess electron and its radial distribution function are shown in Figure 1. The model Hamiltonian was also used in conjunction with the stabilization method[33] to search for a p-type temporary anion of C_{60}. These calculations locate a p-type temporary anion at −0.01 eV. For the other three fullerene systems, multiple nonvalence correlation-bound anion states are identified (see Table 1).

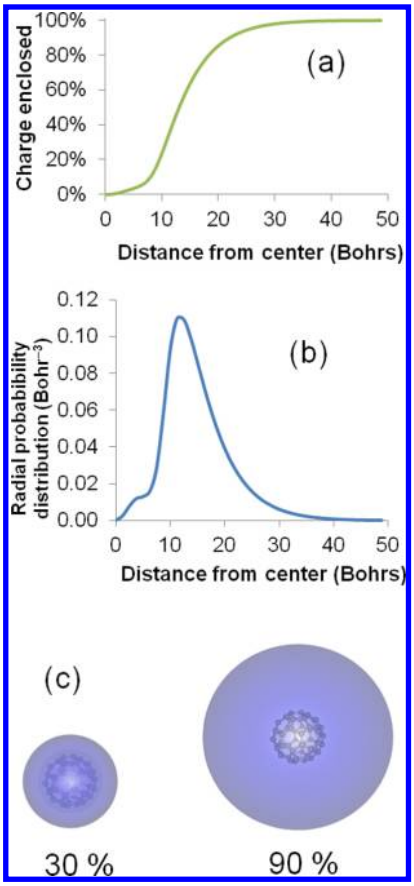

Figure 1. Charge distribution of the nonvalence correlation-bound s-type anion state of C_{60} calculated using the model potential. Panel (a) shows the charge enclosed as a function of the distance from the center of C_{60} while panel (b) depicts the radial distribution of the excess electron. Panel (c) illustrates the orbital occupied by the excess electron at isosurfaces containing 30 and 90% of the charge.

For the C_{60} dimer the calculations were carried out for a 19 Bohr center-to-center separation of the molecules. This distance was chosen to match the experimentally observed distance between the monomers of the C_{60} dimer on the Cu(111) surface.[8] The most stable nonvalence correlation-

dx.doi.org/10.1021/nl5016574 | Nano Lett. 2014, 14, 4602−4606

Table 1. EBEs (eV) of Nonvalence Correlation-Bound Anion States of Selected Fullerenes

C_{60}	$(C_{60})_2$	C_{240}	$C_{60}@C_{240}$
0.13(s)	0.25($s\sigma_g$)	0.70(s)	0.56(s)
−0.01(p)	0.10($s\sigma_u$)	0.38(p)	0.33(p)
	0.06($p\pi_u$)	0.28(s)	0.29(s)
	0.01($p\sigma_g$)	0.15(d)	0.16(d)
		0.02(p)	

bound anion state of $(C_{60})_2$ is calculated to have an EBE of 0.25 eV and corresponds to the plus combination of the s-type nonvalence correlation-bound anion states of the isolated molecules (denoted as $s\sigma_g$). In addition, there are nonvalence correlation-bound anion states that correspond to $s\sigma_u$, as well as to $p\pi_u$ and $p\sigma_g$ superatom molecular orbitals (see Figure 2).

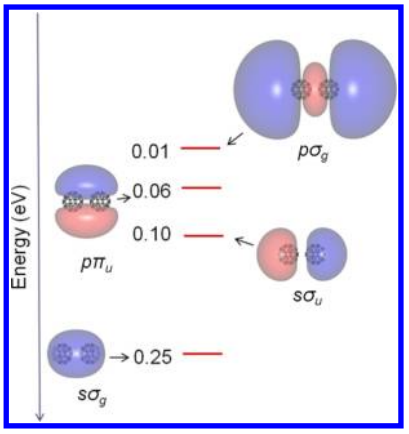

Figure 2. Energies of the nonvalence correlation-bound anion states of $(C_{60})_2$ at a center-to-center separation of 19 Bohrs between the fullerene molecules. The orbital isosurfaces correspond to 80% of the charge of the excess electron enclosed.

The calculated splitting between the lowest energy $s\sigma_g$ and $s\sigma_u$ states of $(C_{60})_2$ is 0.15 eV, which is in reasonable agreement with the experimentally observed splitting of 0.26 eV for the C_{60} dimer on Cu(111). We note also that the bound $p\pi_u$ and $p\sigma_g$ anion states of $(C_{60})_2$ can be viewed as arising from the p-type temporary anion state of C_{60}.

For C_{240}, the calculations give five nonvalence correlation-bound anion states that are 1s, 1p, 2s, 1d, and 2p in nature. The most stable of these is the 1s state that is predicted to be bound by 0.70 eV, compared to 0.13 eV EBE of the s-state of C_{60} anion. As seen from Figure 3, for the lowest energy nonvalence correlation-bound anion of C_{240} most of the charge density of the excess electron is localized inside the cage. The second most stable nonvalence correlation-bound anion of C_{240}, labeled 1p, has significant charge both inside and outside of the cage. The three higher-lying anion states have most of the charge density of the excess electron outside the cage. The existence of nonvalence correlation-bound anion states with significant charge either inside or outside of the cage is closely related to the "+" and "−" states of graphene discussed by Silkin et al.[15]

Given the localization of the excess electron associated with the 1s nonvalence correlation-bound anion state of C_{240}, one could question the validity of the model Hamiltonian approach to this species. It is relevant to note, therefore, that we have previously demonstrated in the case of water clusters that our model Hamiltonian approach successfully described both the

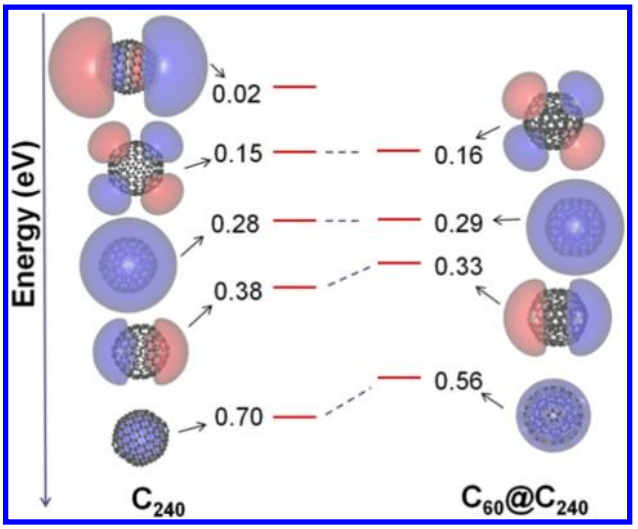

Figure 3. Energies of the nonvalence correlation-bound anion states of C_{240} and $C_{60}@C_{240}$. The orbital isosurfaces correspond to 80% of the charge of the excess electron enclosed.

very diffuse as well as more localized nonvalence correlation-bound anion states of these clusters.[13] We note also that over 82% of the charge of the excess electron of the 1s state of C_{240} is outside the region defined by the inner and outer van der Waals shells of the molecule. For these reasons, we are confident that the model Hamiltonian is providing a semi-quantitatively correct description for the wave function and EBE of this species.

We also characterized the nonvalence correlation-bound anion states of $C_{60}@C_{240}$. As expected, the lowest energy nonvalence correlation-bound anion state of $C_{60}@C_{240}$ is appreciably less stable than that of C_{240} itself. This is essentially an "excluded volume" effect. On the other hand, the second-lowest energy s-type and the lowest energy p-type and d-type nonvalence correlation-bound anion states of C_{240} for which the charge density of the excess electron is located predominantly outside the C_{240} cage are relatively unaffected by the encapsulation of the C_{60} molecule.

In order to better understand the impact of the encapsulation of the C_{60} on the nonvalence correlation-bound states of C_{240}, we plot in Figure 4 the radial distribution functions of the two lowest energy s-states of C_{240} and $C_{60}@C_{240}$. As expected, the lowest energy s-state of $C_{60}@C_{240}$ has more charge outside of the C_{240} cage than does the corresponding state of C_{240}.

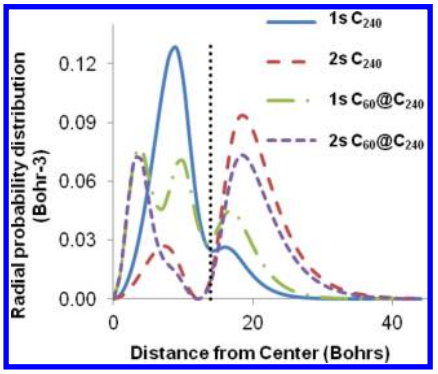

Figure 4. Radial distribution functions of the *s*-type states of C_{240} and $C_{60}@C_{240}$. The dashed vertical line at 13.9 Bohrs denotes the distance from the center of the C_{240} cage to one of the C atoms of C_{240}.

dx.doi.org/10.1021/nl5016574 | Nano Lett. 2014, 14, 4602−4606

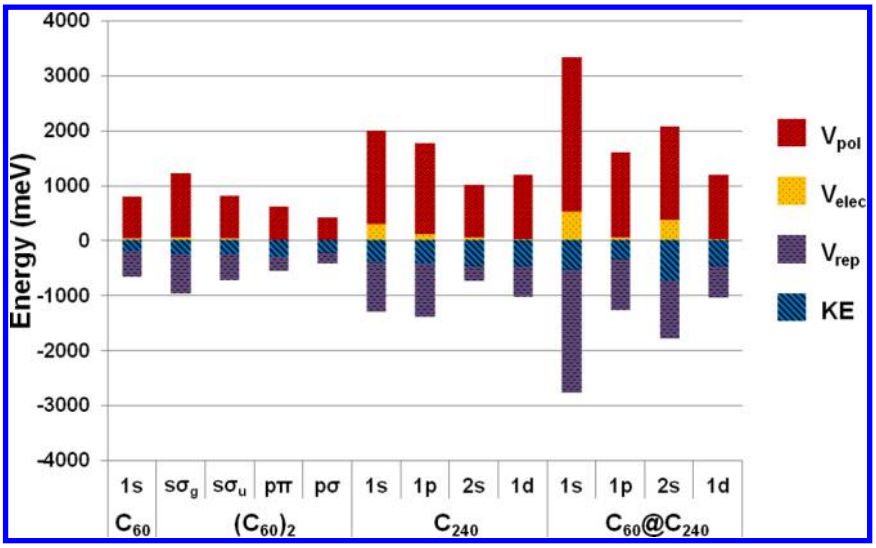

Figure 5. Electrostatic, repulsion, polarization, and kinetic energy (KE) contributions to the EBEs of the nonvalence correlation-bound anion states of C_{60}, $(C_{60})_2$, C_{240}, and $C_{60}@C_{240}$.

However, the presence of the C_{60} also causes a shift of charge density to near the inner wall of the enclosed C_{60}.

We have also separated the net EBE of each nonvalence correlation-bound anion state considered into kinetic energy, electrostatics, repulsive, and polarization contributions, summarizing the results in Figure 5. For the 1s anion of C_{60}, the calculations give, respectively, values of −191, −476, 42, and 755 meV for the kinetic, repulsion, electrostatic, and polarization contributions to the EBE. (Here we are continuing to use the convention that positive contributions are stabilizing.) The confinement of the electron thus introduces sizable kinetic energy and repulsive contributions. The attractive electrostatic interaction is quite small, and the stability of the s-type anion of C_{60} is mainly due to the sizable (755 meV) polarization interaction that more than compensates for the energetic cost of confinement. The much stronger binding of the lowest energy s-type state of C_{240} compared to that of C_{60} is largely a consequence of the much greater polarization contribution of the latter. Not surprisingly, the individual contributions to the EBE of the lowest s-type state of $C_{60}@C_{240}$ are very different from the corresponding results for the 1s state of C_{240} with the electrostatics, repulsive, and polarization contributions all being much larger in magnitude in the former. More surprising is the finding that the individual contributions to the EBE of the 2s anion state of $C_{60}@C_{240}$ are very different from those of the 2s anion state of C_{240} itself. This is a consequence of an increase in charge density near the inner "wall" of C_{60} of $C_{60}@C_{240}$.

In this work, we have introduced a one-electron model Hamiltonian for describing the nonvalence correlation-bound anion states of fullerenes. The model includes both point-inducible dipoles and charge-flow polarization, both of which are important for describing the polarization interaction of the excess electron with the fullerenes. The model is applied to C_{60}, C_{240}, $(C_{60})_2$, and $C_{60}@C_{240}$. Whereas C_{60} is found to have a single s-type nonvalence correlation bound anion state, the larger systems have multiple nonvalence correlation-bound anion states. For the C_{60} dimer, at a separation of 19 Bohrs the model potential gives a splitting of 0.15 eV between the lowest energy $s\sigma_g$ and $s\sigma_u$ nonvalence correlation bound anion states as compared to the 0.26 eV splitting measured experimentally for $(C_{60})_2$ on the Cu(111) surface. The discrepancy between the calculated and measured splittings suggests that the interactions of the C_{60} molecules with the Cu(111) surface, present in the experimentally studied system but lacking in the gas-phase dimer investigated here, significantly impact the splitting. In the case of C_{60}, we also located a p-like resonance, which is unbound by only 0.01 eV. The model Hamiltonian developed in this work has been incorporated in our in-house PISCES code, which is freely available upon request. It can be readily extended to treat excess electrons interacting with graphene flakes and carbon nanotubes.

■ ASSOCIATED CONTENT

Supporting Information

Details on $\alpha^{\text{fullerene}}$, $\mathbf{M}^{\text{ind}}$, and constrained charge-flow equations. This material is available free of charge via the Internet at http://pubs.acs.org.

■ AUTHOR INFORMATION

Corresponding Author

*E-mail: jordan@pitt.edu.

Notes

The authors declare no competing financial interest.

■ ACKNOWLEDGMENTS

This work was carried out the under NSF Grant CHE1111235. V.K.V. also acknowledges the DeWitt C. Clapp fellowship from Department of Chemistry, University of Pittsburgh. The calculations were carried out on computers in the University of Pittsburgh's Center for Simulation and Modeling. We thank Professor Petek for stimulating discussions on his work on C_{60} on metal surfaces.

■ REFERENCES

(1) Sommerfeld, T.; Bhattarai, B.; Vysotskiy, V. P.; Cederbaum, L. S. *J. Chem. Phys.* **2010**, *133*, 114301.

(2) Bezchastnov, V. G.; Vysotskiy, V. P.; Cederbaum, L. S. *Phys. Rev. Lett.* **2011**, *107*, 133401.

(3) Voora, V. K.; Cederbaum, L. S.; Jordan, K. D. *J. Phys. Chem. Lett.* **2013**, *4*, 849−853.

(4) Vysotskiy, V. P.; Cederbaum, L. S.; Sommerfeld, T.; Voora, V. K.; Jordan, K. D. *J. Chem. Theory Comput.* **2012**, *8*, 893−900.

(5) Voora, V. K.; Jordan, K. D. *J. Phys. Chem. A* **2013**, DOI: 10.1021/jp408386f.
(6) Vondrak, T.; Zhu, X.-Y. *J. Phys. Chem. B* **1999**, *103*, 3449−3456.
(7) Dougherty, D. B.; Feng, M.; Petek, H.; Yates, J. T.; Zhao, J. *Phys. Rev. Lett.* **2012**, *109*, 266802.
(8) Feng, M.; Zhao, J.; Petek, H. *Science* **2008**, *320*, 359−362.
(9) Zhu, X.-Y.; Dutton, G.; Quinn, D. P.; Lindstrom, C. D.; Schultz, N. E.; Truhlar, D. G. *Phys. Rev. B* **2006**, *74*, 241401.
(10) Feng, M.; Shi, Y.; Lin, C.; Zhao, J.; Liu, F.; Yang, S.; Petek, H. *Phys. Rev. B* **2013**, *88*, 075417.
(11) Nooijen, M.; Bartlett, R. J. *J. Chem. Phys.* **1995**, *102*, 3629−3647.
(12) Warshel, A.; Karplus, M. *J. Am. Chem. Soc.* **1972**, *94*, 5612−5625.
(13) Voora, V. K.; Ding, J.; Sommerfeld, T.; Jordan, K. D. *J. Phys. Chem. B* **2013**, *117*, 4365−4370.
(14) Sommerfeld, T.; DeFusco, A.; Jordan, K. D. *J. Phys. Chem. A* **2008**, *112*, 11021−11035.
(15) Silkin, V. M.; Zhao, J.; Guinea, F.; Chulkov, E. V.; Echenique, P. M.; Petek, H. *Phys. Rev. B* **2009**, *80*, 121408.
(16) Craes, F.; Runte, S.; Klinkhammer, J.; Kralj, M.; Michely, T.; Busse, C. *Phys. Rev. Lett.* **2013**, *111*, 056804.
(17) Granger, B. E.; Král, P.; Sadeghpour, H. R.; Shapiro, M. *Phys. Rev. Lett.* **2002**, *89*, 135506.
(18) Zamkov, M.; Woody, N.; Shan, B.; Chakraborty, H. S.; Chang, Z.; Thumm, U.; Richard, P. *Phys. Rev. Lett.* **2004**, *93*, 156803.
(19) Mayer, A. *Phys. Rev. B* **2007**, *75*, 045407.
(20) Mayer, A.; Astrand, P.-O. J. *Phys. Chem. A* **2008**, *112*, 1277−1285.
(21) Jensen, L.; Schmidt, O. H.; Mikkelsen, K. V.; Åstrand, P.-O. J. *Phys. Chem. B* **2000**, *104*, 10462−10466.
(22) Jensen, L.; Åstrand, P.-O.; Mikkelsen, K. V. *Int. J. Quantum Chem.* **2001**, *84*, 513−522.
(23) Chen, J.; Martínez, T. J. *Chem. Phys. Lett.* **2007**, *438*, 315−320.
(24) Chen, J.; Martínez, T. J. J. *Chem. Phys.* **2009**, *131*, 044114.
(25) Finch, C.; Popple, R.; Nordlander, P.; Dunning, F. *Chem. Phys. Lett.* **1995**, *244*, 345−349.
(26) Alberg, M.; Bawin, M.; Brau, F. *Phys. Rev. A* **2005**, *71*, 022108.
(27) Weber, J. M.; Ruf, M.-W.; Hotop, H. *Z. Phys. D: At., Mol. Clusters* **1996**, *37*, 351.
(28) Gumbs, G.; Balassis, A.; Iurov, A.; Fekete, P. *Sci. World J.* **2014**, *2014*, 726303.
(29) Stone, A. *J. Chem. Theory Comput.* **2005**, *1*, 1128−1132.
(30) Stone, A. *The Theory of Intermolecular Forces*, 2nd ed.; OUP: Oxford, 2013.
(31) Light, J. C.; Carrington, T. *Adv. Chem. Phys.* **2007**, 263−310.
(32) Sommerfeld, T.; Choi, T.-H.; Voora, V. K.; Jordan, K. D. Pittsburgh InfraStructure for Clusters with Excess ElectronS, PISCES; www.pisces.pitt.edu (accessed 06.09.2014).
(33) Hazi, A. U.; Taylor, H. S. *Phys. Rev. A* **1970**, *1*, 1109−1120.